

# The Protective of hUC- MSCs Derived Exosomes on Pulmonary Vascular Remodeling in Experimental Pulmonary Hypertension

**Wan Jiang**

Shandong University Cheeloo College of Medicine

**Xiaoli Liu**

Shandong University School of Medicine: Shandong University Cheeloo College of Medicine

**Susu Li**

Shandong University Cheeloo College of Medicine

**Junfu Wang**

Shandong First Medical University - Tai'an Campus

**Kailin Li**

Shandong University School of Medicine: Shandong University Cheeloo College of Medicine

**Qian Xin**

Shandong University School of Medicine: Shandong University Cheeloo College of Medicine

**Jue Wang**

Shandong University School of Medicine: Shandong University Cheeloo College of Medicine

**Chao Sun**

Shandong University Cheeloo College of Medicine

**yun luan** (✉ [luanyun@sdu.edu.cn](mailto:luanyun@sdu.edu.cn))

Shandong University School of Medicine: Shandong University Cheeloo College of Medicine

<https://orcid.org/0000-0002-4744-6160>

---

## Research

**Keywords:** PH, Vascular remodeling, hUC-MSC-EXO, BMP

**Posted Date:** May 5th, 2021

**DOI:** <https://doi.org/10.21203/rs.3.rs-482285/v1>

**License:**   This work is licensed under a Creative Commons Attribution 4.0 International License.

[Read Full License](#)

---

# Abstract

Pulmonary hypertension (PH) is a life-threatening disease, so far no effective method for it. Therefore, the main aim of the present study was to investigate the protective effect of exosomes derived from human umbilical cord mesenchymal stem cells (hUC-MSCs) on PH vascular remodeling and reveal the underlying mechanism. We established monocrotaline-induced PH (MCT-PH) rats and hypoxia induced pulmonary artery smooth muscle cells (H-PASMC) model in vivo and vitro. Exosomes derived from hUC-MSCs (hUC-MSC-EXO) were administration, respectively. Post-operation, our results showed that hUC-MSC-EXO significantly reduced the right ventricular systolic pressure (RVSP) and the right ventricular hypertrophy index (RVHI), inhibited pulmonary vascular remodeling. Furthermore, the hypoxia-induced PASMC proliferation was obviously inhibited in vitro. More-importantly, the results showed that the protein expression levels of BMPR2, BMP-4 and BMP-9 were significantly increased, but the levels of nuclear factor- $\kappa$ B (NF- $\kappa$ B) p65 and bone morphogenetic protein (BMP) antagonists Gremlin-1 were significantly decreased in hUC-MSC-EXO than that in MCT-PH and hypoxia-induced PASMC groups in vivo and vitro, respectively. Taken together, this present study provided the firm information for the use of this new method in treatment of PH, and the mechanism was associated with regulation of BMP signaling pathway.

## Introduction

Pulmonary hypertension (PH) is a life-threatening disease, characterized by pulmonary vascular remodeling and right ventricular failure[1,2]. So far, there is no effective treatment for it and the mortality rate is still high. Our previous study showed that intravenous delivery of mesenchymal stem/stromal cell (MSC) could improve monocrotaline (MCT)-induced experimental PH vascular remodeling and right ventricular impairments[3,4]. However, the efficacy of MSC-based therapies has been increasingly attributed to the paracrine secretion, particularly exosome. Exosome, a subset of extracellular vesicles, are thought to function primarily as intercellular communication vehicles to transfer bioactive lipids, proteins and nucleic acids between cells to elicit biological responses in recipient cells.

Recent studies suggested that exosome secreted by mesenchymal stem cells is a promising potential target for new therapies of PH[5-7]. However, the molecular mechanisms are not fully understood.

A large number of reports [8-10] showed that excessive proliferation of pulmonary artery smooth muscle cells (PASMCs) is an important pathogenesis in PH vascular remodeling process. Bone morphogenetic protein type II receptor (BMPR2) is a key factor in the process of PH pulmonary remodeling occurs[11,12]. BMPR2 levels in pulmonary vascular was significant reduced in non-genetic forms of PH. About 70% of heritable and 20% of idiopathic PH cases have the BMPR2 *gene* mutations. BMPs are multifunctional proteins that regulate cells proliferation, differentiation, and apoptosis, which bind and activate heteromeric complexes of type I and type II receptors. BMPs and there receptors plays a major role in pulmonary hypertension. Type II receptors (BMPR2) significantly decreased in patients with primary PH and in animal models induced by monocrotaline, chronic hypoxia or transgenic mice [13,14]. BMP4 could regulate the complex receptor signaling pathways associated with BMPR2 in distal PASMCs during the

process of pulmonary arterial remodeling in PH [15]. BMP9 not only protected pulmonary arterial endothelial cells from apoptosis and promotes vascular stability, but also increased BMP2 gene expression [16]. Nuclear factor- $\kappa$ B, an inflammation-related transcription factor, upregulation of NF- $\kappa$ B signaling can promote vascular intima formation, smooth muscle cells proliferation and remodeling [17]. Report shows that pulmonary arterial endothelial cell apoptotic and endothelial to mesenchymal transition (Endo-MT) events caused by NF- $\kappa$ B signaling pathways in the lungs has significant correlation with BMP pathway [18], however, the basic mechanism has not been fully understood.

Here, the purpose of this experiment was to observe the protective effect of hUC-MSC-EXO against PH and explore the mechanism was related to the up-regulation the BMP signal pathway.

## Methods

### Animal

All animals received humane care in compliance with the Guide for the Care and Use of Laboratory Animals published by the US National Institute of Health. Also, all experiments were approved by the Institutional Animal Care and Use Committee of Shandong University. The monocrotaline-induced PH (MCT-PH) rat model has been well-established extensively. All animals were anaesthetized by isoflurane inhalation (1.5-2%) and then euthanized by cervical dislocation.

### Preparation of exosomes

Healthy pregnant women umbilical cord collection from obstetrics of our hospital. We stated that the experiment process conform to the principles outlined in the declaration of Helsinki and investigators have obtained the informed written consent before enrolling participants in clinical trials. Isolation of MSCs from human umbilical cord (hUCMSCs) Wharton's Jelly with some modification[10].The immunotyping characterization of hUCMSCs occurred at passage 3-4 using human specific antibodies CD34, CD45, CD73, CD90, CD105, HLA-DR (BD Biosciences Pharmingen, San Diego, CA) by a fluorescence-activated cell sorter (FACS, BD FACSAria II). Adipogenic, osteogenic and chondrogenic differentiation capacity of T of hUCMSCs was performed by special medium (Cyagen US Inc), and then stained with Alizarin Red-S, Toluidine blue and Oil Red-O, respectively. The plates were seen using microscope, and images were taken from them.

When reached 90% confluences, the adherent cells were incubated in DMEM with 5% exosome-depleted FBS for 24 h, and 5-8 passages hUC-MSC were used for experiments. The conditioned medium was centrifuged at 4°C at 300 g for 10 min at 2000 g for 10 min and finally at 10 000 g for 30 min to remove the cells and debris, followed by centrifugation of the supernatant at 100 000 g at 4°C for 1 h. hUC-MSC-EXO was resuspended in PBS and filtered with a 0.22  $\mu$ m microfiltration membrane, centrifuged again in PBS at 100,000 g for 1 h to collect the exosomes. The protein concentration of hUC-MSC-EXO was determined using a bicinchoninic acid (BCA) assay kit.

The morphology of MSC-EXO was examined using a transmission electron microscope (TEM) according to the manufacturer's instructions. Briefly, the prepared exosomes were stained with phosphotungstic acid solution and then performed under a Hitachi-9000 TEM system. Western blotting was used to detect the protein markers of hUC-MSC-EXO, such as CD63, CD81, TS101 and ALIX.

### **Animals experimental design**

Sprague-Dawley rats PH model was established by a single subcutaneous injection of MCT(60 mg/kg; Sigma, St. Louis, MO, USA) [15]. Three weeks later, the animals received were given at a dose of 50 µg/day hUC-MSC-EXO or an equal volume of culture medium (hUC-MSC-CM) via tail vein injection once daily for 3 days, starting 1 weeks after the last series MCT injections[5]. The protein concentration of hUC-MSC-EXO was determined by a BCA assay kit, and 50 µg protein in 100 µl PBS was used. The rats were randomly divided into 4 groups (n=10): Control, MCT-PH, hUC-MSC-EXO, and hUC-MSC-CM groups. The animals were evaluated at 4 weeks after MCT injection.

### **Hemodynamic and the right ventricular hypertrophy assessment**

Post-operation, all animals were anaesthetized by isoflurane inhalation (1.5-2%) and then euthanized by cervical dislocation. Hemodynamic data were recorded eight weeks after operation as previously described with some modifications. Via femoral vein access, a 5F Swan-Ganz catheter (Edwards Lifesciences Corp, Irvine, CA) was advanced into the pulmonary artery for determination of heart rate (HR), systemic blood pressure (SBP) and right ventricular systolic pressure (RVSP). For assessment of right ventricular hypertrophy, the left ventricle (LV) plus the septum (LV+S) were harvested, and the weight ratio of the RV to LV+S weight calculated to quantify the right ventricular hypertrophy. The index by the formula:  $RV/(LV+S) \times 100$ .

### **Histology and immunology analysis**

Post-operation, the lung and heart were quickly harvested and fixed in 4% paraformaldehyde and embedded in paraffin, the serially sectioned at a thickness of 4-5 µm were stained with hematoxylin-eosin (H&E). To evaluate pulmonary artery structural remodeling, the vascular wall thickness (WT), vascular external diameter (ED), vascular wall area (WA) and total vascular area (TA) to calculate WT% (WT/ED) and WA% (WA/TA) were measured as our previously[6,7]. Fibrosis area of heart and lung were analyzed by Masson's trichrome staining, and then the sections were captured as digital images. Images were taken with an Eclipse 90i microscope (Nikon, Tokyo, Japan).

Immunofluorescence were used to analysis the expression of CD31 and α-SMA. Briefly, after blocking with 5% bovine serum albumin for 30 min at room temperature, the lung sections were incubated overnight at 4°C with anti-CD31 (AF3628) and α-SMA (ab21027) antibodies. Then, sections were further incubated with a antibody for 2 h at room temperature. Subsequently, the sections were followed by 1-h incubation in the dark with florescence isothiocyanate-conjugated secondary antibody. Images were

taken with ZEISS LSM800 confocal microscope (Tokyo, Japan). All experiments were performed by two examiners blinded to treatment assignment.

## **Cell experiment**

Rats PSMCs were purchased from Procell Life Science&Technology Co.,Ltd. (Wuhan, China), and cultured in special culture medium (Procell, China) supplemented with 100 U $\mu$ g/ml of penicillin, 100 IU/ml streptomycin, and 10% (vol/vol) fetal bovine serum (FBS) at 37°C in a humidified normoxia condition (21% O<sub>2</sub>, 5% CO<sub>2</sub>, 74% N<sub>2</sub>) or a hypoxic cells incubator in hypoxia condition (3% O<sub>2</sub>, 5% CO<sub>2</sub>, 92% N<sub>2</sub>). At different time points, hypoxia-induced pulmonary vascular smooth muscle cells (H-PASMCs) were treatment with hUC-MSC-EXO (100  $\mu$ g/ml). The experimental were randomly divided into 3 groups: Normal, H-PASMCs, and hUC-MSC-EXO groups.

## **Cell proliferation assays**

Cell proliferation was monitored using a cell counting kit (CCK)-8 assay. Briefly, PSMCs were seeded into 96-well plates at about at a density of 5 $\times$ 10<sup>3</sup> cells/well. The cells were subjected to hypoxia with or without hUC-MSC-EXO at different time points, and then CCK-8 reagent (10  $\mu$ l) was added to each each well and further incubated for 3 h. The absorbance was measured at 450 nm in a spectrophotometer. Analysis of cellular deoxyribonucleic acid (DNA) content discloses frequencies of cells in G0/1, S and G2/M phase by Flow Cytometry used Cell Cycle and Apoptosis Analysis Kit (Roche Diagnostics, Indianapolis, IN, USA) according to the manufacturer's instructions.

## **Real-time PCR analysis**

Quantitative real-time polymerase chain reaction (qRT-PCR) analysis was performed to detect the relative expression of CD31 and  $\alpha$ -SMA using genespecific primers as described previously. Briefly, total RNA in lung tissues or PAEC was extracted using RNeasy kit (Qiagen, Valencia, CA). ABI Prism 7900 sequence detection system software (version 2.2) was used to analysis the data were, and  $\beta$ -actin was used as an internal control for input RNA. The primers were designed by the Primer Express software package.

## **Western blot analysis**

The tissues and cells protein concentration was detected using a BCA assay kit, lysates were separated by polyacrylamide gel electrophoresis (PAGE) and electro-transferred onto a polyvinylidene fluoride (PVDF), the embranes were blocked in 5% skimmed milk-Tris-buffered saline plus Tween-20 solution and incubated with primary antibodies, respectively, overnight at 4°C. The primary antibody-labeled membranes were then treated with the horseradish peroxidase (HRP)-conjugated goat anti-rabbit secondary antibody to IgG at room temperature for 1.5h. The bound antibodies were visualized by using an enhanced chemiluminescence reagent (Millipore, Billerica, Ma, USA) followed by Bio-Rad Image Lab™. Data was expressed as the relative density of the protein normalized to GAPDH. Primary antibodies of CD9 (ab92726), CD63 (Invitrogen,10628D), CD81(MA5-32333), TSG101(MA5-32463), ALIX(ab186429),  $\alpha$ -

SMA (ab21027), BMPR2 (ab170206), NF- $\kappa$ B-p65 (ab16502), p-NF- $\kappa$ B-p65 (ab86299), BMP4 (ab39973), BMP9 (ab35088), ID1(ab168256), Gremlin (sc-18274), PCNA (ab92552), Cyclin D1(MA5-15512), P27Kip1(ab32034), and GAPDH (ab181602) were used, respectively.

## Statistical analysis

All data are expressed as mean $\pm$ SD. Comparisons of parameters between 2 groups were made with unpaired Student t test. Comparisons of parameters among 3 groups were made with one-way analysis of variance (ANOVA), followed by the Scheffe *post hoc* test. Statistical analysis was carried out by using the SPSS 19.0 software.  $P < 0.05$  was regarded as significant statistical difference.

## Results

### Characterization of hUC-MSCs and hUC-MSC-EXO

Flow cytometric analysis demonstrated that the majority of hUC-MSCs expressed high levels of the CD73, CD90, and CD105 markers, whereas CD34, CD45 and HLA-DR markers were relatively absent (Figure 1A). According to the Alizarin Red-S, Oil Red-O and Toluidine blue staining, it was recognized that hUC-MSCs have the ability to differentiate into osteocytes, adipocytes and cartilage (Figure 1B).

Characterization of the shape and size of MSC-EXO was carried out by transmission electron microscope, the range of hUC-MSC was between 50-150 nm in size ( Figure 1C). The protein expression of hUC-MSC-EXO markers was detected by western blot, the results showed that an enrichment of CD9, CD63, CD81, ALIX and TSG101 levels in hUC-MSC-EXO (Figure 1D).

### hUC-MSC-EXO attenuated MCT-induced PH pulmonary artery remodeling

In the present study, no animals in control and hUC-MSC-CM groups were dead of acute pulmonary edema within the first week of the MCT administration, however, two animals in MCT-PH group and one in hUC-MSC-EXO group were dead, three replacement animals was utilized following the same procedure and treatment. Post-operation, we evaluate MCT-induced lung and heart injury by detecting RVSP and right ventricular hypertrophy index  $RV/(LV+S)$ , as shown in Figure 2A, a significant increased of RVSP and  $RV/(LV+S)$  in MCT-PH and hUC-MSC-CM groups as compared with control ( $P < 0.05$ ), these indicated that we successfully established PH model in rats. However, the increased of RVSP and  $RV/(LV+S)$  were significantly inhibited by hUC-MSC-EXO ( $P < 0.05$ ). There was no significantly different in HR and SBP between groups ( $P > 0.05$ ).

Lung sections were stained with H&E and Masson's trichrome was used to analysis the medal thickness of pulmonary arterial walls and the degree of fibrosis. As shown in Figure 2B, WT% and WA% of muscular arteries with an external diameter of 15 to 50  $\mu$ m were significantly increased in MCT-PH and hUC-MSC-CM groups than that in control, but notably decreased in hUC-MSC-EXO group ( $P < 0.05$ ). The same results also showed in Masson's stained, Figure 2C and 2D showed that hUC-MSC-EXO treatment reduced heart and lung fibrosis than that in MCT-PH or hUC-MSC-CM group ( $P < 0.05$ ).

## Effect of hUC-MSC-EXO on MCT-Induced vascular proliferation

To determine whether MCT-Induced vascular proliferation, the smooth muscularization cells marker  $\alpha$ -SMA and endothelial cell marker protein marker CD31 were detected by RT-PCR, western blot and double immunofluorescence staining for. Our results showed that the protein and mRNA expression of  $\alpha$ -SMA was significantly increased, but CD31 was significantly decreased in MCT-PH and hUC-MSC-CM groups than that in control, however, which were significantly repaired in hUC-MSC-EXO group as compared with MCT-PH and hUC-MSC-CM groups ( $P < 0.05$ , Figure 3A-3C). On the other hand, our results also showed that hUC-MSC-EXO could inhibition of MCT-induced pulmonary vascular endothelial-to-mesenchymal transition (Endo-MT). Furthermore, western blot results showed that the protein expression of proliferating cell nuclear antigen (PCNA) and cell-cycle regulatory protein D1 (Cyclin D1) was significantly decreased, but the protein expression of cell cycle inhibitor P27<sup>kip1</sup> was significantly increased in hUC-MSC-EXO group than that in MCT-PH and CM groups (Figure 4D,  $P < 0.05$ ).

## Effect of hUC-MSC-EXO on PASMC proliferation

The PASMC proliferation were measured by CCK8 when cells treatment with a hypoxia or normoxia condition in the presence or absence of hUC-MSC-EXO fraction for 24 h, 48 h and 72h. The results indicated that the proliferation was significantly reduced in hUC-MSC-EXO group as compared with hypoxic exposure groups (Figure 4A,  $P < 0.05$ ). Cells were harvested and analyzed by flow cytometry at hypoxic exposure 48 h to measured the change of cell cycle. Our results showed that the percentage of G0/G1 phase was significantly increased in hUC-MSC-EXO group as compared with the hypoxic group, while the parentage of G2/M+S phase was significantly decreased, makes cells stay at rest and promotes the transition from S phase to mitosis, the G2 phase ( $P < 0.05$ , Figure 4B).

The cells proliferation was also detected by immunofluorescence in *vitro*. The results showed that the protein expression of proliferating cell nuclear antigen Ki67 was obviously decreased in hUC-MSC-EXO treatment group as compared with hypoxia group (Figure 4C,  $P < 0.05$ ). Furthermore, western blot results showed that the protein expression of Cyclin D1 was significantly decreased, but the protein expression of P27<sup>kip1</sup> was significantly increased in H-PASMCs group than that in control. However, hUC-MSC-EXO administration could significantly restore these results than that in H-PASMCs group (Figure 4D,  $P < 0.05$ ).

## Effect of hUC-MSC-EXO on BMP signaling pathway

Our results of western blot showed that BMPR2 signaling, characterized by rising of BMPR2, BMP4, BMP9 and ID1 expression were significantly lower, BMP antagonists Gremlin-1 was higher in MCT-PH and hypoxia groups as compared with control, but an obviously up-regulation of BMPR2, BMP4, BMP9 and ID1, down-regulation of Gremlin-1 in hUC-MSC-EXO group than those in MCT-PH and hypoxia groups respectively in *vivo* and *vitro* ( $P < 0.05$ , Figure 5A and 5B).

NF- $\kappa$ B is a key transcriptional regulator factor, plays a key role in the process of vascular remodeling in a variety of physiological and pathophysiological states. Reports have previously showed a direct

association of NF- $\kappa$ B with BMP signaling in the lungs of MCT-PH, inhibition of NF- $\kappa$ B attenuated PH by regulating BMPR2-ID axis gene. Here, our western blot and immunofluorescence results showed that the protein expression expression of NF- $\kappa$ B p65, p-NF- $\kappa$ B p65 and the ratio between phospho and total NF- $\kappa$ B p65 (p-p65/p65) were down-regulation in hUC-MSC-EXO group than in PH and hypoxia groups ( $P < 0.05$ , Figure 5C and 5D).

## Discussion

Pulmonary hypertension (PH) is a kind of refractory rare lung diseases, distal pulmonary arterial remodeling is the characteristic of it[19,20]. The pathogenesis of PH is not clear yet, and no effective therapy is available for it. Previous studies[21,22,18] suggested the exosomes isolated from mesenchymal stem cells has the potential to inhibition of vascular remodeling in PH. In the present study, our data confirmed that hUC-MSC-EXO could significantly reduce RVSP and RV/(LV +S) as compared with the MCT-PH rats *in vivo* and inhibition of PASMSs proliferation induced by hypoxia *in vitro*, which is considered as a novel potential therapeutic approach for PH.

Bone morphogenetic proteins (BMPs) and their receptors were required for PH-induced right ventricular hypertrophy, which playing an important role in the remodeling of pulmonary resistance vessels in the process of PH occurs[8,23,24]. BMPR2 mutations have been reported in more than 70% of heritable cases of PH and approximately 20% of apparently sporadic cases of idiopathic PH [25,26]. Loss of BMPR 2 or dysfunction of BMP signaling were associated with the occurrence of PH [16]. BMPs involved in a wide range of cell function including proliferation, migration, differentiation, and apoptosis. Mounting evidence indicates that several BMPs, including BMPR2, BMP4 and BMP9 play as an important role during endocrine regulator of pulmonary arterial remodeling, cardiovascular, metabolic, and haematopoietic function [13-16]. BMPR2 signaling as a cause of increased proliferation of PAMSCs playing an important role in the remodeling of pulmonary resistance vessels in PH [25], BMP9 could protect pulmonary arterial endothelial cells from apoptosis and promotes vascular stability, increase BMPR2 gene expression, and further enhancement of BMPR2 signaling.

The induction of inhibitor of DNA binding protein (ID) expression by BMP contributes to its pro-angiogenic response. Regulation of Id proteins by BMPs, with relevance to PH, play an main effect in the smooth muscle cell function . Id family of transcription factors, especially ID1 and ID3 as important functional targets of BMP signaling, are potently regulated by BMP signalling in PAMSCs and might play a complementary and partially redundant role in regulating cell cycling in vascular and other tissues[27]. ID family of transcription factors as important functional targets of BMP signaling, with relevance to PH, both ID1 and ID3 were downregulated in the lungs along with BMPR2 in MCT rats [28,29]. In the present study, our data corroborated with the association of BMPs with PH, the results demonstrate the expression levels of BMP signaling related protein molecules BMP2, BMP4, BMP9, BMPR2 and ID1 were restored when the PH rats were treatment with hUC-MSC-EXO compared with the MCT-PH rats. To further explore the underlying mechanism of hUC-MSC-EXO against PH, here, PAMSC were induced by hypoxia *in vitro* in the presence or absence of hUC-MSC-EXO. The effect of hUC-MSC-EXO on proliferation and

apoptosis abilities of PAMSC were also analyzed, the results showed the protein expression of CyclinD1 was significantly higher, but the the expression of P27 were significantly lower in hUC-MSC-EXO group than that in H-PASMCs group. Therefore, our data provide a strong evidence for the inhibition of hUC-MSC-EXO on PH vascular remodeling.

In PAMSCs, BMPR2 mutation, leads to a proproliferative, apoptosis-resistant cell phenotype, that may contribute to the process of vascular obliteration observed in PH. BMP signaling is tightly regulated by inflammatory mediators/inflammation [30,31]. Inflammatory cytokines are associated with the pathogenesis of PH, inflammatory molecules were significant infiltration of macrophages and accumulation in the mice treated with MCT [32,33]. Inflammatory cytokines stimulation reduced the expression of BMP2 and BMPR2, promote excessive PAMSC proliferation and pulmonary vascular remodeling in the setting of BMPR2 deficiency in PAMSCs [34]. Reports have previously showed a direct association of NF- $\kappa$ B with BMP signaling in the lungs of MCT-PH, inhibition of NF- $\kappa$ B attenuated PH and RVH by regulating BMPR2-ID axis gene in heart[12, 35]. Moreover, we further confirmed that NF- $\kappa$ B signaling were downregulated in the hUC-MSC-EXO group in *vivo* and *vitro*. The present study at least part suggested that mechanism of hUC-MSC-EXO against PH was through inhibition of NF- $\kappa$ B signaling and activation BMP signaling on experimental PH and pulmonary vascular remodeling. Collectively, these data suggested that the mechanism of hUC-MSC-EXO promote apoptosis and inhibit proliferation in *vitro* is likely to be relevant with BMP signaling and maybe associated with anti-inflammatory response .

## Conclusions

The present study demonstrated that hUC-MSC-EXO attenuated PH pulmonary vascular remodeling through increased the vascular remodeling associated BMPR2 signaling pathway.

## Abbreviations

BMP: bone morphogenetic protein; Endo-MT:Endothelial-to-mesenchymal transition; Exo: Exosomes; hUC-MSCs: Human umbilical cord mesenchymal stem cells; MCT: Monocrotaline; NF- $\kappa$ B: nuclear factor- $\kappa$ B; PAMSC: Pulmonary arterial smooth muscle cells; PH: Pulmonary hypertension; RT-PCR: Real-time polymerase chain reaction; RVSP:the right ventricular systolic pressure, RVHI:the right ventricular hypertrophy index.

## Declarations

### Acknowledgement

The authors are grateful to the Central Research Laboratory of the Second Hospital of Shandong University for technical assistance and generous support.

### Authors' contributions

Authors' contributions:YL designed the research and oversaw the writing of the manuscript; WJ, XLL, KLL, QX, JW and CS performed the experiments and wrote the manuscript; WJ, XLL,SSL, JFW, and YL analyzed the data. All authors have read and approved the manuscript.

## **Funding**

This project was supported by the by the National Natural Science Foundation of China (grant no. 81500042), Natural Science Foundation of Shandong Province (ZR2020MH001), Youth Interdisciplinary Innovation Science Fund of Shandong University (2020QNQT019), the Science and Technology Development Project of Jinan Medical and Health (202019126 and 201907001), Science and Technology Development Project of Shandong Province (2019GSF107093).

## **Availability of supporting data**

All data generated in this study are included in this manuscript.

## **Ethical Approval and Consent to participate**

All participants were provided with written informed consent at the time of recruitment. And this study was approved by the Ethics Committee of the Second Hospital of Shanodng University.

## **Consent for publication**

Not applicable.

## **Competing interests**

The authors declare that they have no competing interests.

## **References**

1. Lambert M, Capuano V, Boet A, Tesson L, Bertero T, Nakhleh MK, et al. Characterization of kcnk3-mutated rat, a novel model of pulmonary hypertension. *Circ Res*. 2019;125(7):678–95.
2. Wang J, Yu M, Xu J, Cheng Y, Li X, Wei G, et al. Glucagon-like peptide-1 (GLP-1) mediates the protective effects of dipeptidyl peptidase IV inhibition on pulmonary hypertension. *J Biomed Sci*. 2019;26(1):6.
3. Luan Y, Zhang X, Kong F, Cheng GH, Qi TG, Zhang ZH. Zhang. Mesenchymal stem cell prevention of vascular remodeling in high flow-induced pulmonary hypertension through a paracrine mechanism. *Int Immunopharmacol*. 2012;14(4):432–7.
4. Luan Y, Zhang ZH, Wei DE, Zhao JJ, Kong F, Cheng GH, Wang YB. Wang. Implantation of mesenchymal stem cells improves right ventricular impairments caused by experimental pulmonary hypertension. *Am J Med Sci*. 2012;343(5):402–6.

5. Aliotta JM, Pereira M, Wen S, Dooner MS, Del Totto M, Papa E, et al. Exosomes induce and reverse monocrotaline-induced pulmonary hypertension in mice. *Cardiovasc Res*. 2016;110(3):319–30.
6. Lee C, Mitsialis SA, Aslam M, Vitali SH, Vergadi E, Konstantinou G, et al. Exosomes mediate the cytoprotective action of mesenchymal stromal cells on hypoxia-induced pulmonary hypertension. *Circulation*. 2012;126:2601–11.
7. Hogan SE, Rodriguez Salazar MP, Cheadle J, Glenn R, Medrano C, Petersen TH, Ilagan RM. Mesenchymal stromal cell derived exosomes improve mitochondrial health in pulmonary arterial hypertension. *Am J Physiol Lung Cell Mol Physiol*. 2019;316(5):L723-37.
8. Humbert M, Sitbon O, Chaouat A, Bertocchi M, Habib G, Gressin V, et al. Survival in patients with idiopathic, familial, and anorexigen-associated pulmonary arterial hypertension in the modern management era. *Circulation*. 2010;122(2):156–63.
9. de Man FS, Handoko ML, Vonk-Noordegraaf A. The unknown pathophysiological relevance of right ventricular hypertrophy in pulmonary arterial hypertension. *Eur Respir J*. 2019;53(4). pii: 1900255.
10. Kurakula K, Sun XQ, Happé C, da Silva Goncalves Bos D, Szulcek R, Schalij I, et al. Prevention of progression of pulmonary hypertension by the Nur77 agonist 6-mercaptopurine: role of BMP signaling. *Eur Respir J*. 2019;54(3). pii: 1802400.
11. Li L, Wei C, Kim IK, Janssen-Heininger Y, Gupta S. Inhibition of nuclear factor- $\kappa$ B in the lungs prevents monocrotaline-induced pulmonary hypertension in mice. *Hypertension*. 2014;63(6):1260–9.
12. Hurst LA, Dunmore BJ, Long L, Crosby A, Al-Lamki R, Deighton J, et al. TNF $\alpha$  drives pulmonary arterial hypertension by suppressing the BMP type-II receptor and altering NOTCH signalling. *Nat Commun*. 2017;8:14079.
13. Atkinson C, Stewart S, Upton PD, Machado R, Thomson JR, Trembath RC, Morrell NW. Primary pulmonary hypertension is associated with reduced pulmonary vascular expression of type II bone morphogenetic protein receptor. *Circulation*. 2002;105(14):1672–8.
14. Dewachter L, Adnot S, Guignabert C, Tu L, Marcos E, Fadel E, Humbert M, Darteville P, Simonneau G, Naeije R, Eddahibi S. Bone morphogenetic protein signalling in heritable versus idiopathic pulmonary hypertension. *Eur Respir J*. 2009;34(5):1100–10.
15. Zhang Y, Wang Y, Yang K, Tian L, Fu X, Wang Y, Sun Y, Jiang Q, Lu W, Wang J. BMP4 increases the expression of TRPC and basal [Ca<sup>2+</sup>]<sub>i</sub> via the p38MAPK and ERK1/2 pathways independent of BMPRII in PSMCs. *PLoS One*. 2014;9(12):e112695.
16. Long L, Ormiston ML, Yang X, Southwood M, Gräf S, Machado RD, Mueller M, Kinzel B, Yung LM, Wilkinson JM, Moore SD, Drake KM, Aldred MA, Yu PB, Upton PD, Morrell NW. Selective enhancement of endothelial BMPRII with BMP9 reverses pulmonary arterial hypertension. *Nat Med*. 2015;21(7):777–85.
17. Wang YY, Luan Y, Zhang X, Lin M, Zhang ZH, Zhu XB, Ma Y, Wang YB. Proteasome inhibitor PS-341 attenuates flow-induced pulmonary arterial hypertension. *Clin Exp Med*. 2014;14(3):321–9.
18. Li L, Wei C, Kim IK, Janssen-Heininger Y, Gupta S. Inhibition of nuclear factor- $\kappa$ B in the lungs prevents monocrotaline-induced pulmonary hypertension in mice. *Hypertension*. 2014;63(6):1260–9.

19. Pham T, Nisbet L, Taberner A, Loisel D, Han JC. Pulmonary arterial hypertension reduces energy efficiency of right, but not left, rat ventricular trabeculae. *J Physiol*. 2018;596(7):1153–66.
20. Han JC, Guild SJ, Pham T, Nisbet L, Tran K, Taberner AJ, Loisel DS. Left-ventricular energetics in pulmonary arterial hypertension-induced right-ventricular hypertrophic failure. *Front Physiol*. 2018;8:1115.
21. Rabinovitch M, Guignabert C, Humbert M, Nicolls MR. Inflammation and immunity in the pathogenesis of pulmonary arterial hypertension. *Circ Res*. 2014;115(1):165–75.
22. Song Y, Jones JE, Beppu H, Keaney JF Jr, Loscalzo J, Zhang YY. Increased susceptibility to pulmonary hypertension in heterozygous BMP2-mutant mice. *Circulation*. 2005;112(4):553–62.
23. Hautefort A, Mendes-Ferreira P, Sabourin J, Manaud G, Bertero T, Rucker-Martin C, et al. Bmpr2 mutant rats develop pulmonary and cardiac characteristics of pulmonary arterial hypertension. *Circulation*. 2019;139(7):932–48.
24. Yan L, Cogan JD, Hedges LK, Nunley B, Hamid R, Austin ED. The Y chromosome regulates BMP2 expression via SRY: a possible reason "Why" fewer males develop pulmonary arterial hypertension. *Am J Respir Crit Care Med*. 2018;198(12):1581–3.
25. Rabinovitch M. Molecular pathogenesis of pulmonary arterial hypertension. *J Clin Invest*. 2012;122:4306–13.
26. Morrell NW, Bloch DB, ten Dijke P, Goumans MJ, Hata A, Smith J, Yu PB, Bloch KD. Targeting BMP signalling in cardiovascular disease and anaemia. *Nat Rev Cardiol*. 2016;13(2):106–20.
27. Lowery JW, Frump AL, Anderson L, Di Carlo GE, Jones MT, de Caestecker. MPID family protein expression and regulation in hypoxic pulmonary hypertension. *Am J Physiol Regul Integr Comp Physiol*. 2010;299(6):R1463-77.
28. Ciumas M, Eyries M, Poirier O, Maugendre S, Dierick F, Gambaryan N, Montagne K, Nadaud S, Soubrier F. Bone morphogenetic proteins protect pulmonary microvascular endothelial cells from apoptosis by upregulating  $\alpha$ -B-crystallin. *Arterioscler Thromb Vasc Biol*. 2013;33(11):2577–84.
29. Kumar S, Wei C, Thomas CM, Kim IK, Seqqat R, Kumar R, Baker KM, Jones WK, Gupta S. Cardiac-specific genetic inhibition of nuclear factor- $\kappa$ B prevents right ventricular hypertrophy induced by monocrotaline. *Am J Physiol Heart Circ Physiol*. 2012;302:H1655-66.
30. Morrell NW, Bloch DB, ten Dijke P, Goumans MJ, Hata A, Smith J, et al. Targeting BMP signalling in cardiovascular disease and anaemia. *Nat Rev Cardiol*. 2016;13(2):106–20.
31. Singhatanadgit W, Salih V, Olsen. Bone morphogenetic protein receptors and bone morphogenetic protein signaling are controlled by tumor necrosis factor-alpha in human bone cells. *Int J Biochem Cell Biol*. 2006;38(10):1794–807.
32. Kim CW, Song H, Kumar S, Nam D, Kwon HS, Chang KH, et al. Anti-inflammatory and antiatherogenic role of BMP receptor II in endothelial cells. *Arterioscler Thromb Vasc Biol*. 2013;33(6):1350–9.
33. Yu PB, Deng DY, Beppu H, Hong CC, Lai C, Hoyng SA, et al. Bone morphogenetic protein (BMP) type II receptor is required for BMP-mediated growth arrest and differentiation in pulmonary artery smooth muscle cells. *J Biol Chem*. 2008;283(7):3877–88.

34. Cai P, Kovacs L, Dong S, Wu G, Su Y. BMP4 inhibits PDGF-induced proliferation and collagen synthesis via PKA-mediated inhibition of calpain-2 in pulmonary artery smooth muscle cells. *Am J Physiol Lung Cell Mol Physiol*. 2017;312(5):L638-48.
35. Crosby A, Soon E, Jones FM, Southwood MR, Haghghat L, Toshner MR, et al. Hepatic shunting of eggs and pulmonary vascular remodeling in *Bmpr2*(+/-) mice with schistosomiasis. *Am J Respir Crit Care Med*. 2015;192(11):1355–65.

## Figures

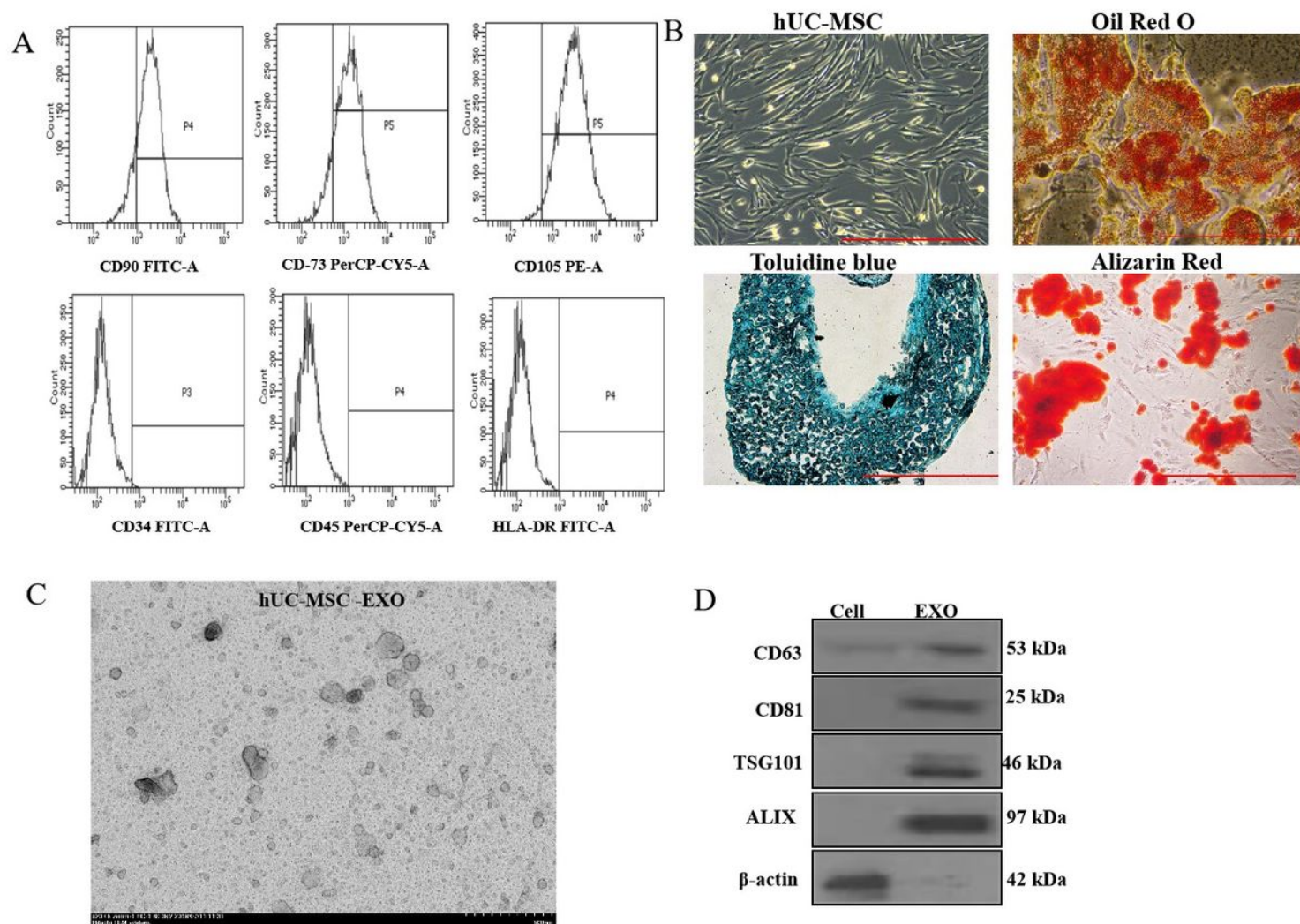


**Figure 1**

Characterization of hUC-MSCs and hUC-MSC-EXO (A) The immunotyping characterization of human umbilical cord (hUC-MSCs) analysis by Flow cytometry analysis. (B) Cell morphology and differentiation ability analysis. (C) Exosomes derived from hUCMSCs detection by transmission electron microscope. (D)The protein expression of markers analysis by western blot.

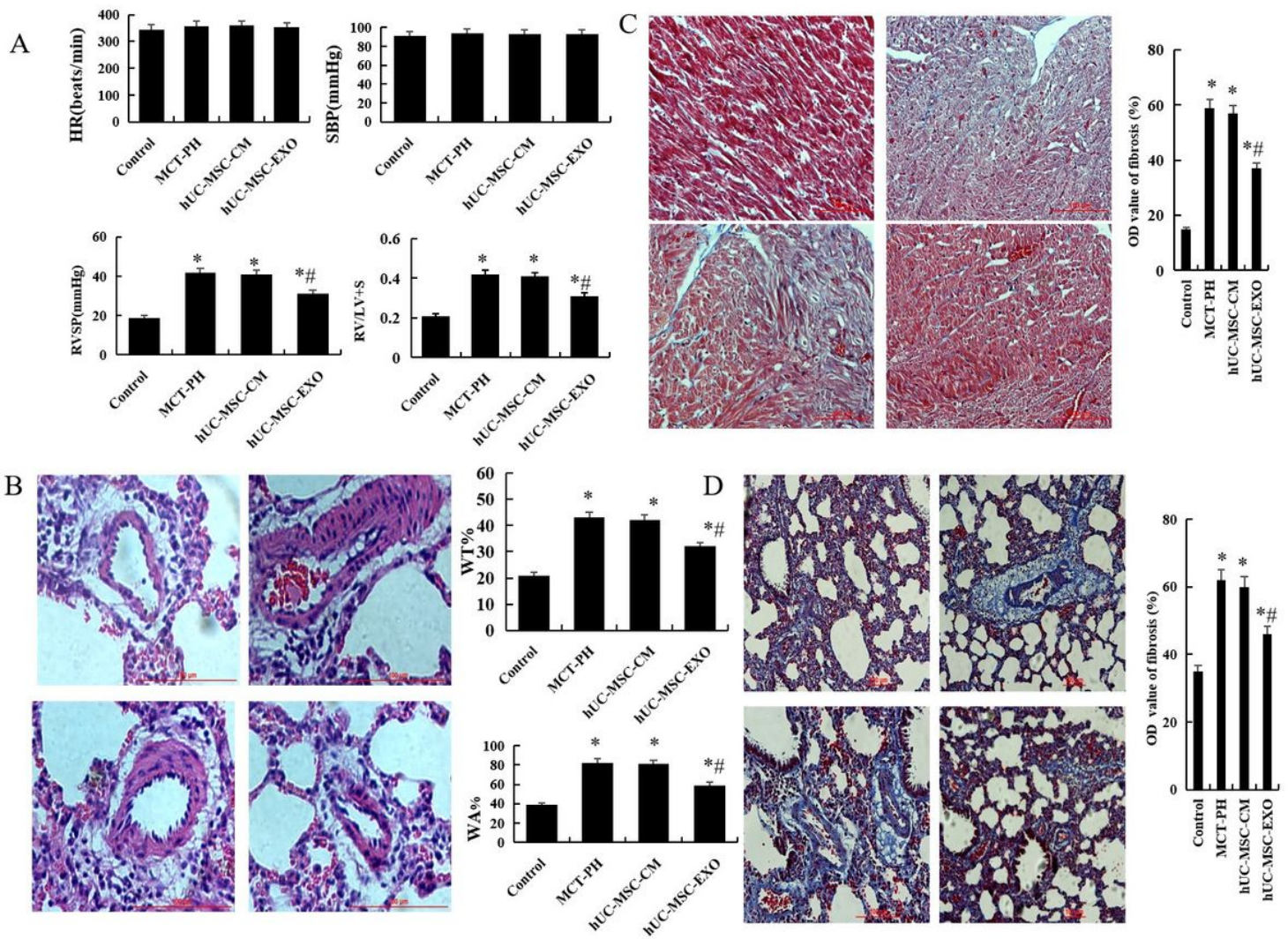


**Figure 2**

Effect of hUC-MSC-EXO on MCT-induced pulmonary hypertension (A) A comparison of the HR, SBP, RVSP and RV/LV+S in each group. (B) Hematoxylin and eosin staining and comparison of the medial thickness of the pulmonary arterial walls in each group. (C) Massons staining and comparison of the OD value in heart (D) Massons staining and comparison of the OD value in lung. Red bar = 100  $\mu$ m. MCT: monocrotaline; HR: heart rate; SBP: systemic blood pressure; RVSP: right ventricular systolic pressure; RV/LV+S: the ratio of right ventricular weight to left ventricle plus septum; WT%: the percent of the vascular wall thickness (WT)/vascular external diameter (ED); WA%: the percent of vascular wall area (WA)/total vascular area (TA); OD: optical density calibration. the data are present as mean  $\pm$  SD; \* $P$ <0.05 and \*\* $P$ <0.01 compared with control group;# $P$ <0.05 compared with MCT-PH.

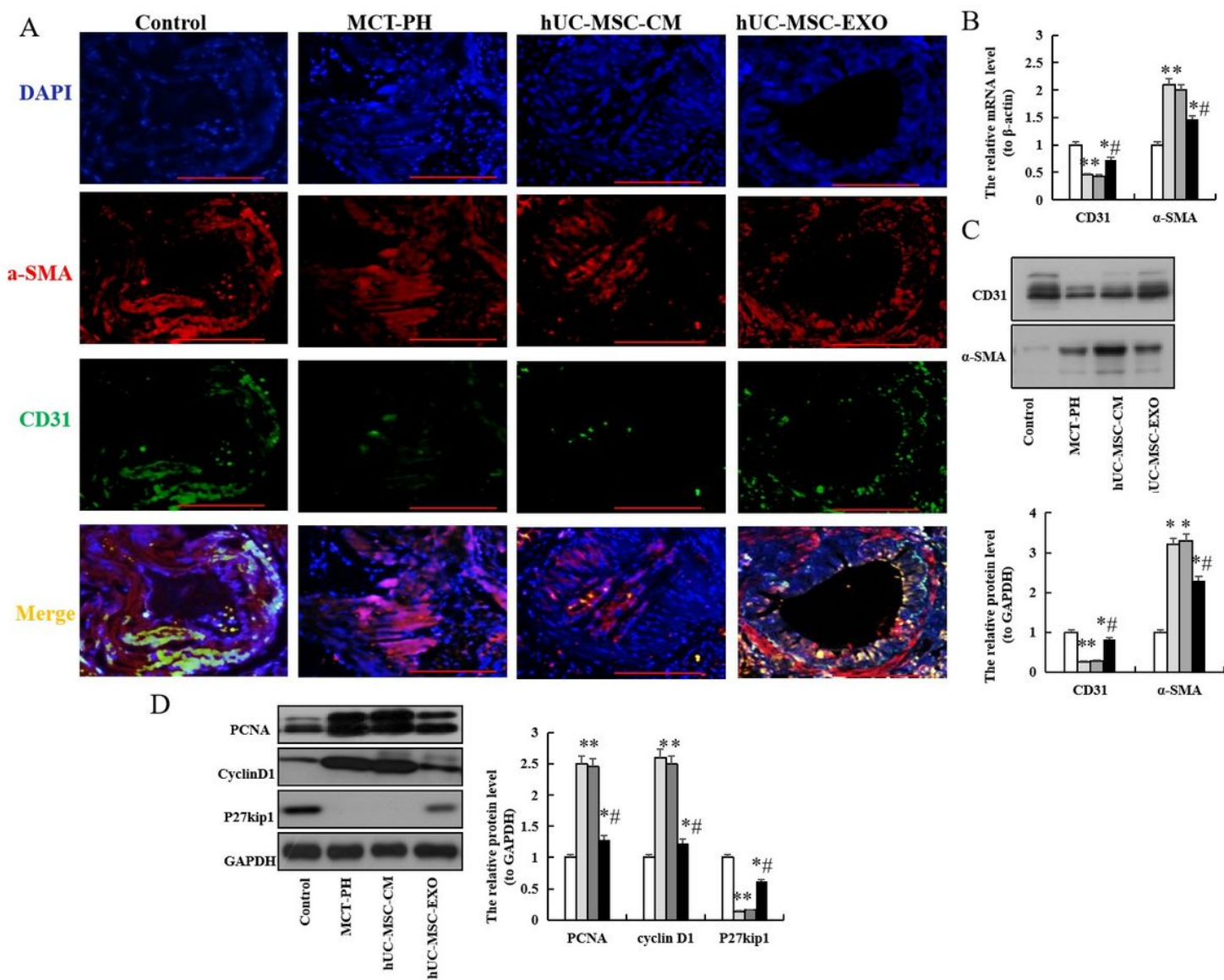


**Figure 3**

Effects of hUC-MSC-EXO on MCT-induced pulmonary artery smooth muscle (A) The expression of  $\alpha$ -smooth muscle actin (a-SMA) and CD31 analyzed by immunofluorescence (B) A comparison of optical density (OD) value in each group. (B) the mRNA level of a-SMA and CD31 by RT-PCR. (C) the protein expression analyzed of PCNA, Cyclin D1 and P27kip1 analysis by western blot. PCNA: proliferating cell nuclear antigen; Cyclin D1: cell-cycle regulatory protein D1; P27kip1: cell cycle inhibitor p27Kip1. the data are present as mean  $\pm$  SD; \* $P$ <0.05 compared with control group; # $P$ <0.05 compared with MCT-PH.

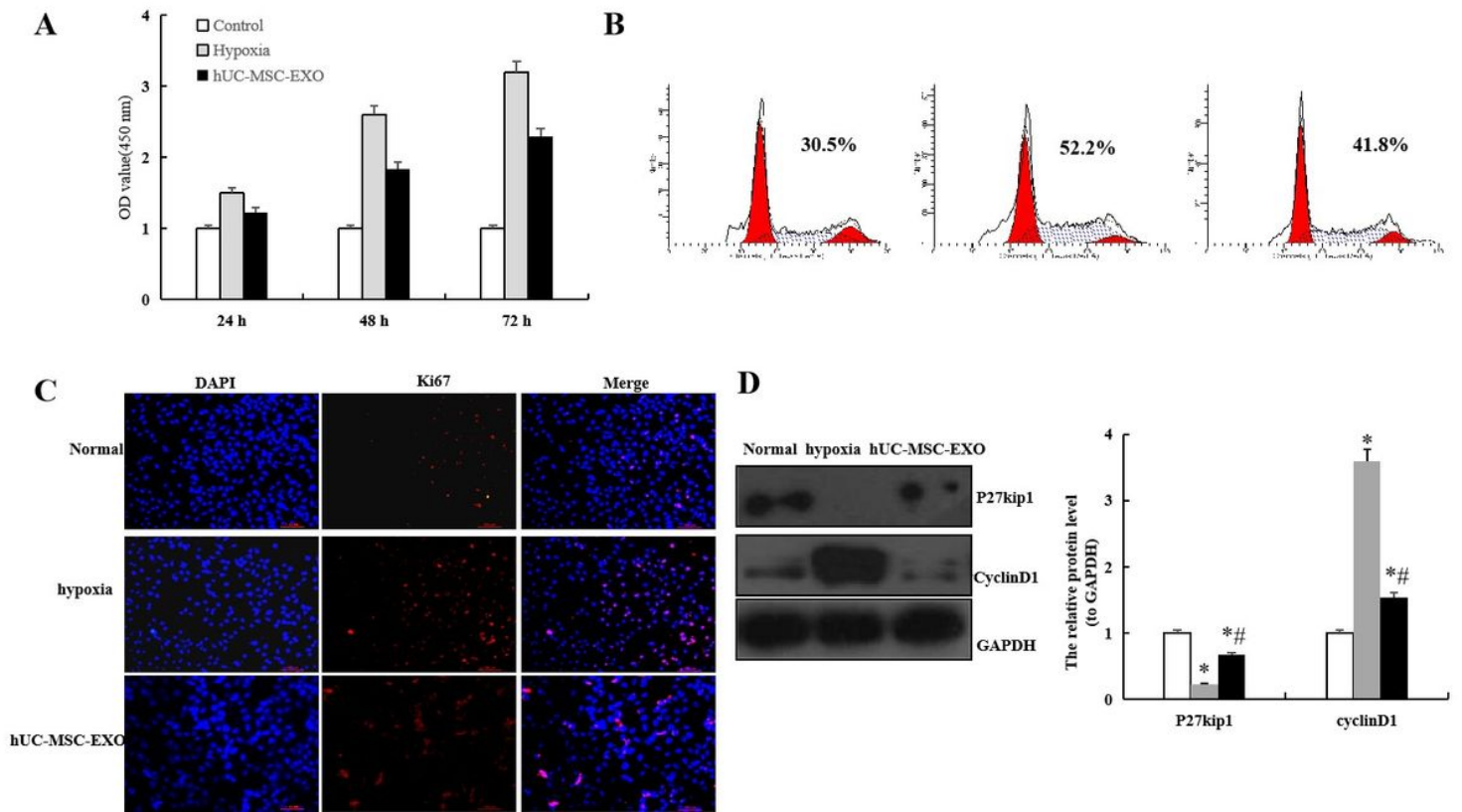


**Figure 4**

Effect of hUC-MSC-EXO on hypoxia-induced PSMCs proliferation (A) CCK8 assay. (B) Cell cycle analysis. (C) Ki67 detected by immunofluorescence. Red bar = 100  $\mu$ m. (D) the protein expression of Cyclin D1 and p27 analysis by western blot. the data are present as mean  $\pm$  SD; \* $P$ <0.05 compared with Normal group; # $P$ <0.05 compared with hypoxia.

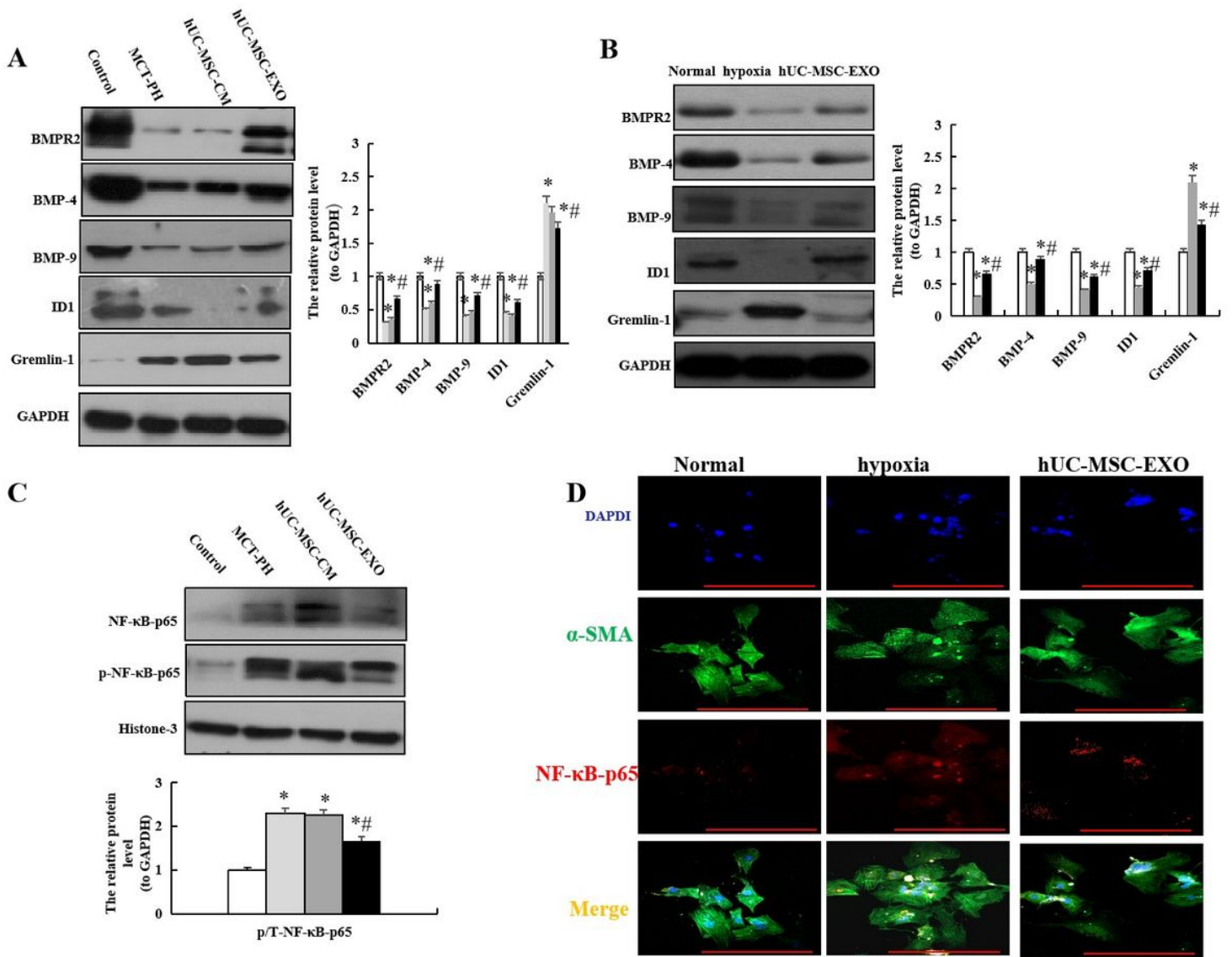


**Figure 5**

Effect of hUCMSC-EXO on BMP signaling pathway (B) (A)the protein expression analysis of BMP signaling pathway in vivo by western blot. (B)the protein expression analysis in vitro by western blot.(C) the protein expression analysis of total and phosphorylation NF-κB p65 signaling pathway in vivo by western blot. (D) the protein expression analysis of NF-κB -p65 in PASMCs by immunofluorescence.the data are present as mean  $\pm$  SD; \*P<0.05 compared with Normal group;#P<0.05 compared with hypoxia.